PERFORMANCE ANALYSIS OF THE PRECISE POINT POSITIONING TECHNIQUE AT BUCU IGS STATION

Constantin-Octavian ANDREI, Senior Research Scientist, Finnish Geodetic Institute (FGI), octavian.andrei@fgi.fi
Dagoberto SALAZAR, Ph.D, Technical University of Catalonia (gAGE/UPC), Spain
Ruizhi CHEN, Professor, Finnish Geodetic Institute (FGI), ruizhi.chen@fgi.fi

***Abstract**: The improved accuracy of precise satellite orbit and clock products in the last decade has attracted interest from the Global Navigation Satellite Systems (GNSS) community to develop a novel positioning technology known as precise point positioning (PPP). PPP uses both pseudorange and carrier phase observations from a single GNSS receiver in order to provide positioning solutions. As these solutions are at centimeter to decimeter-level accuracy on a global scale, PPP can be considered as an efficient alternative to the conventional differential positioning methods. This paper describes an analysis of PPP performance from the accuracy, precision, convergence period, and availability point of view. International GNSS Service (IGS) products are tested. Numerical results will be presented for both static and kinematic mode using dual-frequency data.*

***Keywords:** GNSS, PPP, precise orbit and clock, convergence*

1. Introduction

Global Navigation Satellite System (GNSS) have become a critical component of our modern day infrastructure and services. A GNSS system transmits signals to provide accurate position, velocity and time (PVT) information that is accessible to anyone who has a receiver. There are several different methods for obtaining a position using GNSS technology. The method used depends on the accuracy requirement and the type of the GNSS receiver available.

One such method used by many users and applications implies *absolute positioning* using a stand-alone receiver. This method is based on code-only measurements and the position accuracy is better than 100 m for civilian users and about 15 m for military users (DoD, 2008). These accuracies are mainly due to the effects caused by different GNSS error sources. For many other applications, this accuracy level achieved with GNSS is insufficient. These applications demand for improved accuracy, availability and integrity from the navigation systems. A common way to achieve this is using *differential positioning* that eliminates most of the error sources. Various differential GNSS (DGNSS) techniques have been designed to improve the accuracy of GNSS at different scales: local, regional, global area. There are two main DGNSS techniques according with the type of observations used in estimating the user's position: code-based and carrier phase-based techniques. Code-based DGNSS increases the position accuracy from tens of meters to 2-3 meters or even less, making this technique useful for many civilian applications. Carrier phase-based DGNSS improves the accuracy level down to centimeter and, thus, it is preferred by high accuracy applications. However, all these DGNSS systems suffer from some inconveniences: the requirement of existence of a base or reference station(s); the need for simultaneous

observations at both the reference and the unknown point(s); and the necessity for the target receiver (called rover) to operate in the vicinity of the reference station, given that the error correlation decreases with the distance and then the corrections at the reference station do not replicate the conditions at the rover position. All these inconveniences make DGNSS costly and logistically difficult to operate, especially in remote areas. Thus from the practical point of view, it would be important to have a technique that has logistic and flexible operational characteristics similar to absolute positioning, but at the same time providing accurate position solutions at high-accuracy levels.

During the last decade, the idea to enhance stand-alone code positioning with carrier phase-based positioning has brought interest from the GNSS community. Data collected by a global network of geodetic-quality receivers have been continuously recorded and processed by different International GNSS Service (IGS) Analysis Centers (ACs). As a result, IGS started to provide precise orbit and clock data products necessary for high accuracy point positioning. Processing of undifferenced code pseudo-ranges and carrier phase measurements from a single GNSS receiver, combined with precise satellite orbit and clock products is called Precise Point Positioning (PPP). As no base station is required, PPP eliminates the DGNSS inconveniences. Thus, PPP is logistically simpler than DGNSS and becomes a viable alternative to DGNSS providing almost the same position accuracies (Zumberge et. al, 1997; Kouba and Heroux, 2001). Although PPP does not require a base station, it requires the accurate information of the GNSS satellite orbits and their clocks. This paper investigates the current PPP performance in terms of accuracy, precision, convergence period, and availability. The latest International GNSS Service (IGS) products are tested along for both static and kinematic mode using dual-frequency data.

2. Precise point positioning

There are two mathematical models for dual-frequency precise point positioning. The first model (Kouba and Heroux, 2001) uses the ionosphere-free linear combinations of code and carrier phase observations, but cannot deliver integer-ambiguity-fixed solutions (i.e., it only delivers float solutions). The second model (Gao and Shen, 2002) uses a different observation model based on the ionosphere-free code and phase combination (i.e., the average of code and phase measurement) that reduces code pseudorange noise. Similar to the first model, the second model also cannot solve for the integer ambiguities. The resolution of ambiguity parameters is not performed on point-positioned results from a single receiver because of the receiver and satellite initial not known, non-zero phase biases, although recent works are exploring this possibility (Ge et al., 2008; Laurichesse et al., 2009).

The standard PPP algorithm uses the code pseudorange and carrier phase observations from a single dual-frequency receiver. As a result, the following ionosphere-free data combinations can be formed in order to eliminate the first order ionospheric effects on satellite signals.

$$P_{IF} = \frac{f_1^2 P_1 - f_2^2 P_2}{f_1^2 - f_2^2} = \rho + c(dt - dT) + dorb + drel + dtrop + b_P + b^P + det + dol + derp + dpcv + dmp_{P_{IF}} + \varepsilon_{P_{IF}} \quad (1)$$

$$\Phi_{IF} = \frac{f_1^2\Phi_1 - f_2^2\Phi_2}{f_1^2 - f_2^2}$$
$$= \rho + c(dt - dT) + dorb + drel + dtrop + \lambda_{IF}(N_{IF} + b_\Phi + b^\Phi) + det + dol + derp + dpcv \quad (2)$$
$$+ dpwu_{\Phi_{IF}} + dmp_{\Phi_{IF}} + \varepsilon_{\Phi_{IF}}$$

where P_i is the code measurement on L_i (m); Φ_i is the carrier phase measurement on L_i (m); f_i is the frequency on L_i (MHz); ρ is the geometric range (m); dt is the receiver clock (s); dT is the satellite clock (s); $dorb$ is the satellite orbit error (m); $drel$ is the relativistic delay (m); $dtrop$ is the tropospheric delay (m); b_P, b^P are the receiver and satellite code biases (m); λ is the corresponding wavelength for the ionosphere-free observation (m); N is the integer ambiguity of the ionosphere-free observation (cycle); b_Φ, b^Φ are the receiver and satellite initial phase biases (cycle); det is the solid Earth tide; dol is the ocean loading effect; $derp$ is the polar tide (m); $dpwu$ is the phase wind-up effect (m); $dpcv$ is the range delay due to the satellite and receiver antenna phase center offsets and variations (m); $dmp(.)$ is the multipath effect in the measurement (m) and $\varepsilon(.)$ is the measurement noise (m).

For precise point positioning, a number of additional modeling considerations must be taken into account. The orbit error ($dorb$) and clock error (dT) are removed when precise satellite orbit and clock products are used. The tropospheric delay can be corrected at centimeter level, using existing models and meteorological parameters (Andrei and Chen, 2009). The delay consists of two components: a hydrostatic and a wet component. The hydrostatic zenith delay can be determined with an accuracy of 1.5-3 mm if pressure measurements are available. Conversely, the wet zenith delay is less predictable and, thus, it is considered as unknown parameter by the standard PPP algorithm in the estimation process. The satellite code biases (b^P) are mostly eliminated from the code measurements by using a set of differential code biases (DCBs) between P1 and P2 (Schaer et. al., 1998). If the receiver reports C1 (C/A code) instead of P1, DCBs between P1 and C1 measurements, which are also satellite dependent, should be applied (Jefferson et al., 2001). As to the receiver related DCBs between C1, P1 and P2, they are absorbed by the receiver clock parameter. The antenna phase center offsets and variations ($dpcv$) are corrected using the elevation- and azimuth-dependent corrections obtained via an absolute calibration procedure (Rothacher and Schmid, 2006). There is no mathematical model for correcting the multipath effect (dmp). However, the effect can be minimized through a proper antenna location, carefully designed antennas or receiver design (Seeber, 2003).

As a result of all these above-mentioned considerations, the Eqs (1) and (2) can be simplified to the following equations:

$$P_{IF} = \bar{\rho} + cdt + m_w zwd + \varepsilon_{P_{IF}} \quad (3)$$

$$\Phi_{IF} = \bar{\rho} + cdt + m_w zwd + \lambda_{IF}\overline{N}_{IF} + \varepsilon_{\Phi_{IF}} \quad (4)$$

where $\bar{\rho}$ is the corrected pseudorange between the phase center of the satellite and receiver antenna, m_w is the wet tropospheric mapping factor, zwd is the wet component of the tropospheric delay, and

(5) $$\overline{N}_{IF} = N_{IF} + b_{\Phi} + b^{\Phi}$$

identifies the non-integer ambiguity of the carrier phase.

The unknown vector in the PPP processing includes four types of parameters: the receiver position (dx, dy, dz), the receiver clock (dt), the tropospheric zenith wet delay (zwd), and the float carrier phase ambiguity ($\overline{N}$) terms (equal to the number of satellites observed). The unknown parameters can be estimated sequentially for every epoch using a Kalman filter procedure (Kalman, 1960). The Kalman filter is a set of mathematical equations that provides an efficient recursive mean to estimate the state of a process, in a way that minimizes the mean of the squared error. According to Welch and Bishop (2006), the filter is very powerful in several aspects, supporting estimations of the past, present and future states, and doing so even when the precise nature of the system is unknown. As a result, Kalman filter settings depend on the dynamic conditions, the nature of the parameters and the data sampling interval. From a PPP perspective, the coordinates and receiver clock states are usually modeled as Random Walk or first order Gauss Markov (Axelrad and Brown, 1996; Brown and Hwang, 1997). The long established way for modeling the troposphere is to assign a Random Walk process (Zumberge et. al, 1997; Kouba and Heroux, 2001). The ambiguity states are assumed to be constant if no cycle slips over time. The selection of the suitable stochastic model depends mainly on the application under consideration.

3. Precise orbits and clocks

The precise satellite orbits and clock corrections are tabulated and distributed at 15-minute intervals by different IGS ACs. In addition, IGS has been provided clock corrections in separate independent files with a sampling of 5 minutes. The processing time for a solution with higher sampling rate increases proportionally to the number of additional epochs involved. Therefore, it took a long time until IGS was able to deliver 30s satellite clock corrections. Since GPS week 1406 (December 17, 2006) a combined final product is available with a sampling rate of 30s (Gendt, 2007). Furthermore, one of IGS ACs, namely CODE (Center for Orbit Determination, Bern, Switzerland) has increased the sampling to 5 seconds to support high-rate data processing such as the determination of the precise orbits for low-orbit satellites. Since the start of GPS week 1478 (May 3, 2008), CODE produces 5s satellite clock corrections as the CODE final clock product (Schaer and Dach, 2008). In order to use the 5s clock corrections for 1 Hz applications, they have to be interpolated by the users. Satellite clock corrections at sampling interval of 15 and 5 minutes are obtained from the IGS orbit and clock estimation process, while the satellite clock corrections at the sampling rate of 30 and 5 seconds are obtained based on an efficient phase-consistent interpolation of 5-minute precise clock results using phase time differences (Hugentobler, 2004). Table 1 summarizes the current available precise satellite data. The use of this precise data is divided into four cases according to the satellite clock sampling interval. All precise products have an accuracy of about 2-5 cm for orbits and 0.1 ns for clocks.

Table 1: Type of the precise satellite orbit and clock data

Type of precise data	Data sampling	
	Orbits	Clocks
Case 1, final	15 min	15 min
Case 2, final	15 min	5 min

Case 3, final	15 min	30 sec
Case 4, final	15 min	5 sec

4. Numerical results

In the following section, data processing and analysis are conducted to assess the performance of PPP algorithm from the accuracy, precision, convergence period, and availability point of view. Different satellite data and measurement sampling intervals are tested.

Static positioning results

For a preliminary evaluation of the performance of the PPP technique, a 24 h high-rate (1s) observation dataset collected by the IGS station BUCU (Bucharest, Romania) on January 1, 2010 is selected for the analysis. The BUCU station is equipped with a high-quality geodetic GNSS receiver – LEICA GRX1200GGPRO – connected to a LEIAT504GG antenna. As this test implies static positioning, the dataset is decimated to 30 s in order to match the sampling rate of the final clock products. The final IGS satellite orbit and clock corrections at intervals of 15 minutes and 30 seconds, respectively, are used to remove satellite orbit and clock errors. The P1-C1 differential code biases are used to correct the code measurements as the receiver reports C1(C/A) code instead of P1 (i.e., non cross-correlator receiver type). The estimation scheme for the static positioning is based on Kalman filter evaluation procedure. A white noise process is chosen to describe the stochastic processes for station position, a Random Walk process for the receiver clock bias as well as the tropospheric zenith delay parameters, while constant process is used for the ambiguities parameters. The spectral densities of the estimated parameters are attributed in an empirical way as the rate of change of the parameters (velocity). Therefore, as the station is considered fixed, the spectral density of the station coordinates is considered zero, while the initial position coordinates uncertainty is considered 100m. The receiver clock is assumed to change from epoch to epoch at a rate of 30 m/s and with an initial uncertainty of 300 km. The initial uncertainty of the troposphere zenith delay is assumed to be 0.5 m with a slow change rate of 1 cm/h. The standard deviations for code and carrier phase measurements are considered to be 4.0 m and 0.02 m, respectively. In addition, an elevation-dependent weighting approach is applied to reduce the influence of the low elevation measurements. The receiver antenna phase center offset and variations are obtained using the latest absolute IGS antenna corrections at GPS week 1564. Ocean loading displacements are calculated using ocean tide model GOT00.2, while the rotational deformation due to the polar motion is calculated based on IGS earth rotation parameters.

Figure 1 illustrates the number of satellites and the position dilution of precision (PDOP) after applying a 10 degree elevation mask angle. The average PDOP value is 2.1, while the average number of the processed satellites is 7.6. To assess the quality of the position estimates, the estimated coordinates are compared with the corresponding IGS SINEX solutions for GPS week 1564. The IGS solutions have an accuracy of few millimeters. The results of the static processing are presented in **Figure 2** along with the corresponding statistics. The error values are computed as differences between estimated coordinates and the true values. The large errors in each component in the first hour are due to filter initialization and convergence. The summary statistics for 24 h data set (excluding first 30 min, which is typically the convergence period when satellite corrections at a sampling rate of 30 s are used) show good agreement in the horizontal component with biases smaller than 5 mm and the root-mean-square (rms) factor less than 10 mm. However, the results show -22.4 mm bias in

the vertical component. This value is typical for the PPP technique, and it could be explained by the worse geometry in the vertical direction (high VDOP), as well as inconsistencies in the error models used between the two solutions, such as different ocean loading tide model or higher order earth tide corrections used in the IGS solutions.

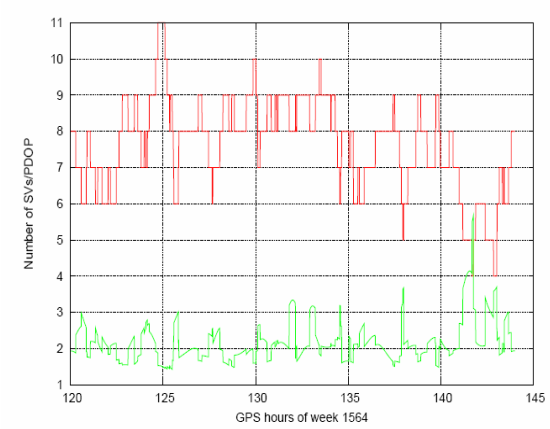

Figure 1: Number of Space Vehicles (SVs) and Position Dilution of Precision (PDOP)

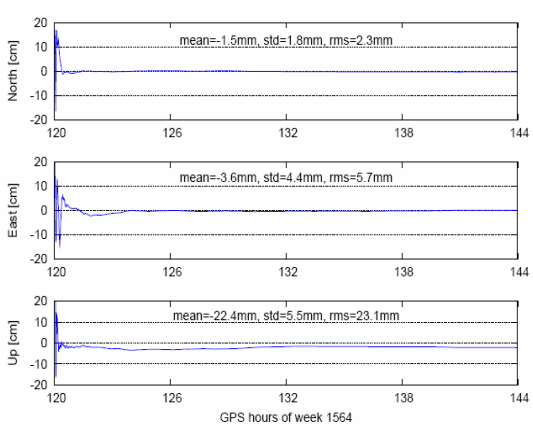

Figure 2: Component errors in the position estimates

Precise satellite data sampling interval testing

The 24h dataset is divided into six 4-hour sessions as shown in Table 2:

Table 2: Session time intervals

Session ID	Session time interval (UTC time)				
	start	End		start	end
1	00:00:00	04:00:00	4	12:00:00	16:00:00
2	04:00:00	08:00:00	5	16:00:00	20:00:00
3	08:00:00	12:00:00	6	20:00:00	24:00:00

During the Kalman filter development, different filter convergence times were observed when using different precise data sampling intervals. The calculation of the convergence time is defined here in a way that no single epoch of positioning errors exceeds the threshold. Accordingly, the convergence time could be less than the average values given in the table because the positional errors can oscillate around the threshold with very small amplitude.

Figure 3 highlights the average convergence time expressed in epochs of observations (1 epoch equals 1 second) for different position components to converge to better than 50, 20 and 10 cm. The effect of precise satellite sampling intervals on the convergence time is large. There is around 50% reduction of the convergence time when using 5-minute satellite clock corrections (i.e., Case 2). In addition, the convergence time is reduced by almost 80% when applying 30 s clock corrections (i.e., Case 3) compared with Case 1 and Case 2. As a result, five sessions of Case 3 achieved horizontal and vertical positioning accuracy better than 10 cm in less than 20 minutes. Furthermore, when using the fourth set of precise data (Case 4), one can notice that the convergence time is almost 30% shorter compared with Case 3. All the sessions for Case 4 achieved vertical positioning accuracy better than 10 cm in less than 10 minutes.

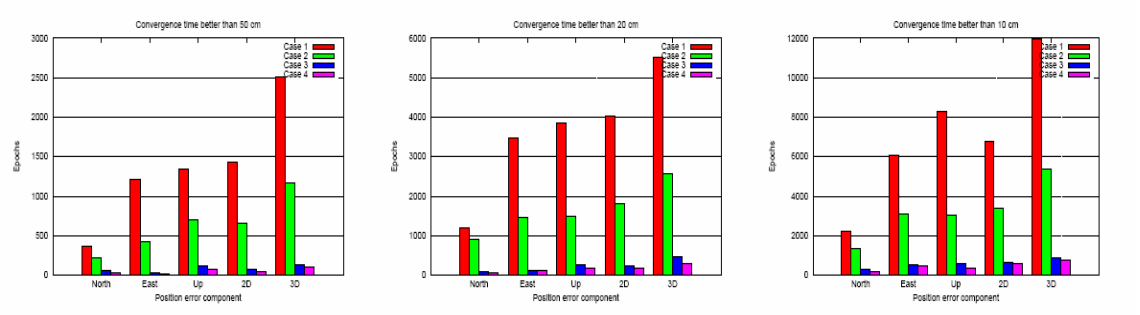

Figure 3: Average convergence time for all sessions when using different precise satellite data sampling intervals.

Figure 4 illustrates the convergence behavior for all sessions when using different precise satellite orbit and clock sampling intervals. For all cases, the convergence time varies from one session to another. This variation is attributed to different satellite geometry during each session and the difference in precise satellite clock data for each satellite. In addition, the same satellite might not have correction values for all the sampling intervals. Nevertheless, the advantage of using high-rate satellite clock corrections is shown in some sessions when considering Case-3 or Case-4. During these sessions, the position component errors do not even exceed the chosen threshold.

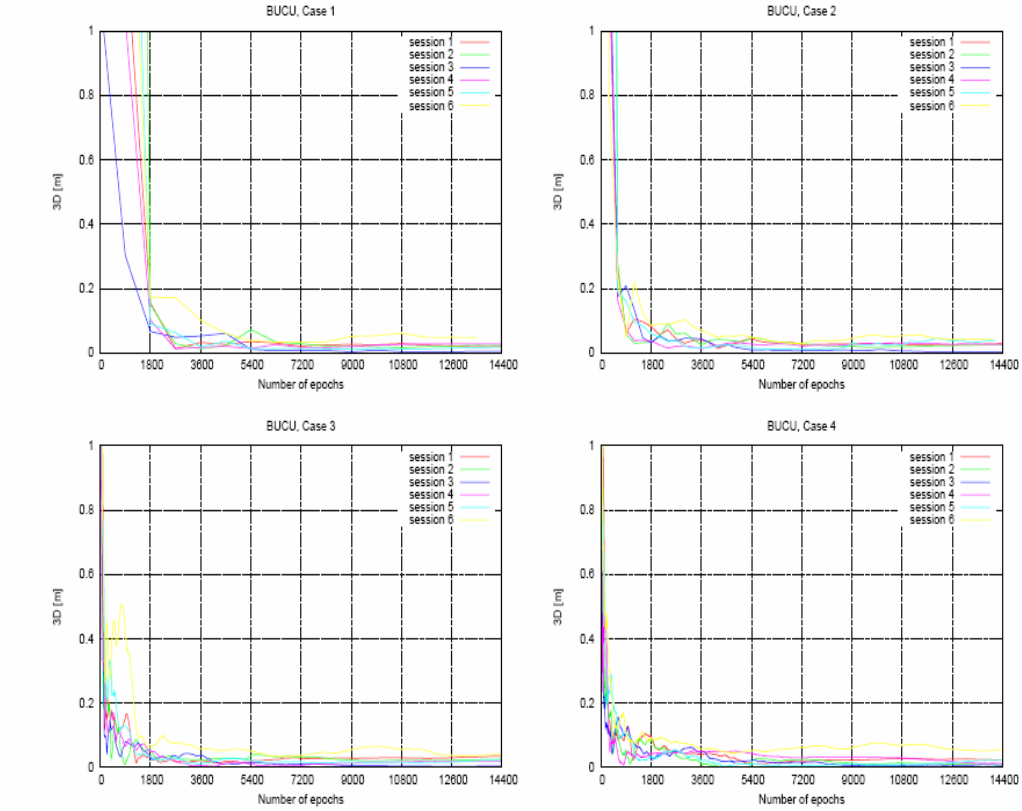

Figure 4: Position error repeatability of the 3D positioning error when using different precise satellite data sampling intervals.

Measurement sampling interval testing

The relationship between the measurement sampling rate and filter convergence time can be observed by comparing the results obtained when using datasets with different observation intervals but same precise data. The 1 Hz dataset used in previous section is down sampled to 5 s, 10 s, and 30 s sampling intervals. The resulting datasets are tested using the same precise data, i.e., Case-4. **Figure 5** shows how the convergence time increases with the measurement sampling interval, as was expected. In this case, the convergence time is defined as the time interval from the initial solution to the time when the standard deviation of the estimated parameters reaches the values observed for one day dataset solution.

Usually in PPP, the orbit and satellite clock corrections are decimated at the corresponding observation time. If, on the other hand, the precise products are interpolated, the error from the orbit interpolation is negligible because the orbits have a very smooth behavior. Conversely, the satellite clock correction interpolation may not be accurate because of the high level of irregularity. This irregularity cannot be attributed to an interpolation strategy defect but to the nature of the satellite clocks. **Figure 6** depicts an example of such irregularities among satellite clock corrections at sampling rate of 30 s, 5 min and 15 min. The 5 s satellite clock corrections are not included in the comparison because they have a different reference time.

Kinematic positioning test

Static observations are used in the kinematic processing mode to evaluate the positioning accuracy obtained with PPP. The estimation scheme used for a kinematic PPP solution is modified accordingly in order to reflect the test dynamics. Thus, the coordinates parameters are treated as changing parameters. The spectral densities of 100 and 25 m^2/s are used for horizontal and vertical component, with an uncertainty of 100 m for the initial coordinates.

The results of the kinematic processing are illustrated in **Figure 7**. The kinematic results reveal a jump in solution accuracy around GPS hour 138. This jump is generated by a complete loss-of-lock for 8 minutes, between epochs 17:37:30 and 17:45:30. The missing data generate a reset of the Kalman filter. As a consequence, a convergence period is needed to resume to centimeter-level accuracy. Table 3 presents the summary statistics for kinematic PPP mode.

The filter residuals (observation minus modeled values), along with associated satellite elevation angles, are shown in **Figure 8**. The code pseudorange RMS factor is 0.63 m with peak-to-peak variations of ±4 m, and the carrier-phase RMS is 0.5 cm with peak-to-peak variations of ±4 cm. These values appear to be reasonable for the particular linear combination of the code and carrier phase combination that they represent.

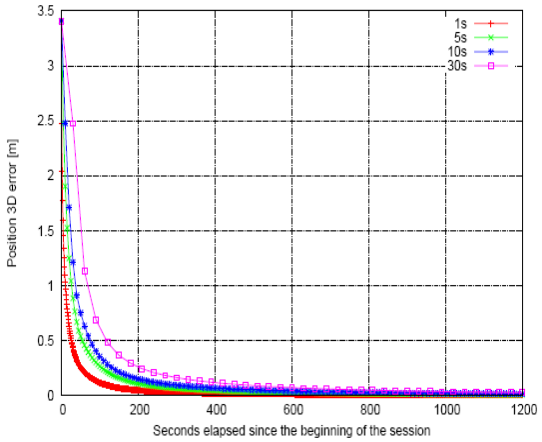

Figure 5: Position solution standard deviation on different datasets with different measurement sampling intervals: 1s (red), 5s (green), 10s(blue), and 30s(magenta)

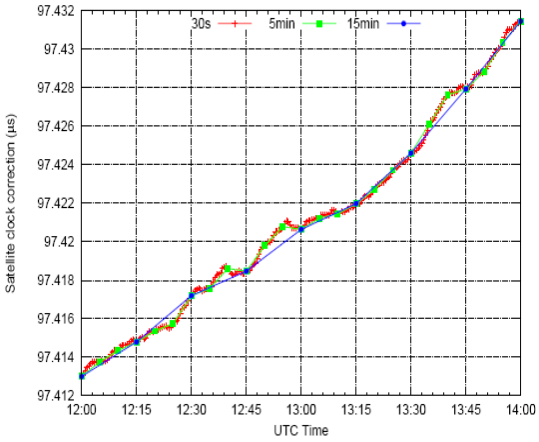

Figure 6: Satellite clock corrections irregularities

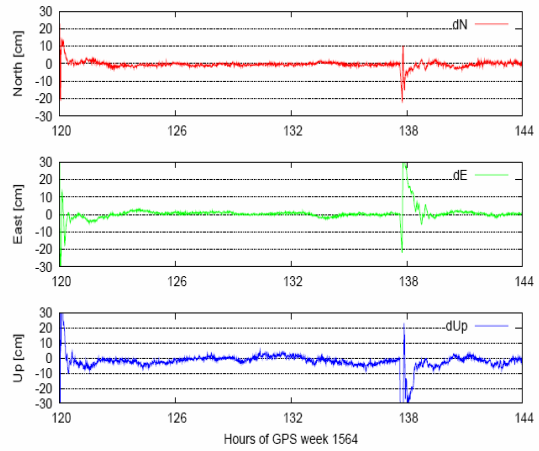

Figure 7: Position component errors for kinematic PPP processing mode

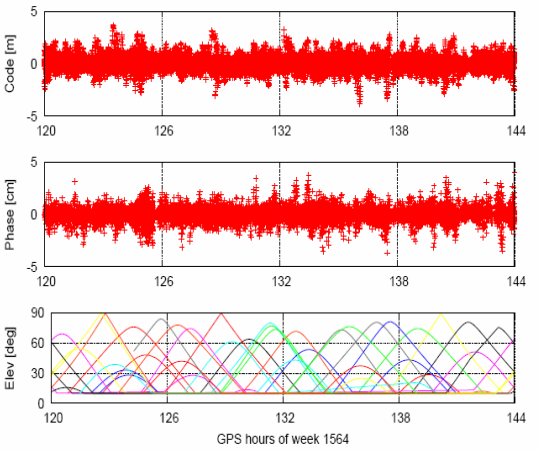

Figure 8: Post-fit residuals and associated elevation angles

Table 3: Summary statistics of kinematic PPP processing mode

Statistics	Position component error (cm)		
	North	East	Up
Mean	-0.5	0.9	-2.4
Std	1.4	4.2	6.3
RMS	1.5	4.2	6.8
Measurement residual RMS (cm)			
Code	63.3	Phase	0.5

5. Conclusions

This paper demonstrates that precise point positioning technique is able to offer centimeter-level accuracies in static mode using the latest IGS satellite orbits and clock products. The PPP static solutions showed very little biases when comparing with IGS final solutions. The small bias presented in the vertical component is typical of this technique and mainly due to the worse vertical geometry and the inconsistencies between the current implementation and IGS models. Kinematic PPP position accuracy was also investigated. The solutions showed that centimeter level accuracy could be obtained. The main problem with kinematic applications is the need of continuous satellite signal tracking. Loss of the minimum required number of available satellites requires processing filter to be reinitialized. Filter reinitialization results in a period of time with over centimeter accuracy solutions until the filter converges.

The main factors that limit the PPP accuracy are the precision of satellite orbits and clocks and the effects of the unmodeled errors. PPP is very fast and efficient way to determine station coordinates. However, currently it is not possible to reach the same accuracy as obtained, for example, from network analysis. This is mainly due to the impossibility to resolve phase ambiguities. Thus, it is expected that the ability to exploit the integer property can further improve the position accuracy.

PPP requires time to achieve centimeter level positioning accuracy. This time is needed by the phase ambiguities to converge to constant values. PPP convergence time depends on a number of factors, such as the constellation geometry, receiver dynamics, measurement quality and sampling rate. The results reported in this paper showed that with high-rate precise satellite clocks, the positioning accuracy better than 10 cm could be achieved in less than 10 minutes. Although for static applications one can use larger measurement sampling intervals such as 30 s, for kinematic applications this may not be an alternative. As such applications require a short convergence time, high-rate 5 s satellite clock corrections are recommended.

Precise point positioning can be used for both static and kinematic data, mainly in post-processing mode. However, the PPP applicability could be extended to real-time applications if there were a way to generate, disseminate and process the precise satellite orbit and clock products in real time.

With the emergence and availability of new satellite systems, such as GLONASS, Galileo or Compass, it is expected that a multi-constellation PPP system would have significant impact on position, accuracy, convergence time and reliability.

6. Acknowledgments

The first author would like to thank the Finnish Geodetic Institute for the financial and technical supports offered in pursuing his doctoral research in Finland. The IGS data and combined solution products (Dow et al., 2005) used in the analysis presented are acknowledged. The authors would also like to acknowledge support from the GPSTk open source project (Tolman et al., 2004).

7. References

1. *Andrei, C-O. and R. Chen (2009). Assessment of time-series of troposphere zenith delays derived from the Global Data Assimilation System numerical weather model. GPS Solutions 13(2):109-117.*
2. *Andrei, C-O. (2010). On Precise Point Positioning as a positioning technique using carrier-phase measurement, Kirkkonummi 2010. 204 pages (submitted for publication).*
3. *Axelrad, P. and Brown, R. G. (1996). GPS Navigation Algorithms. In Parkinson, B. W. and Spilker, J. J., editors, Global Positioning System: Theory and Applications Volume I, volume 163 of Progress in Astronautics and Aeronautics, chapter 9, pages 409–433. American Institute of Astronautics and Aeronautics, Washington, DC.*
4. *Brown, R. G. and Hwang, P. Y. (1997). Introduction to Random Signals and Applied Kalman Filtering . John Wiley & Sons, 3rd edition.*
5. *DoD (2008). Global Positioning System (GPS) Standard Positioning Service (SPS) Performance Standard (PS). published by the Assistant Secretary of Defence for Network and Information Integration [ASD(NII)], 4th Edition.*
6. *Dow, J.M., R.E. Neilan, and G. Gendt (2005). The International GPS Service: Celebrating the 10th anniversary and looking to the next decade. Advances in Space Research, 36(3), 320-326.*
7. *Gao Y., Shen X. (2002). A new method for carrier-phase-based precise point positioning. NAVIGATION: Journal of Institute of Navigation 49(2):109-116*
8. *Ge., M., Gendt., G., Rothacher, M., Shi, C., and Liu, J. (2008). Resolution of GPS carrier-phase ambiguities in Precise Point Positioning (PPP) with daily observations. Journal of Geodesy 82(7):389-399.*
9. *Gendt, G. (2007). Combined IGS clocks with 30 second sampling rate. IGSMAIL-5525, IGS Central Bureau, Pasadena.*
10. *Hugentobler, U. (2004). CODE high rate clocks. IGSMAIL-4913, IGS Central Bureau, Pasadena.*
11. *Jefferson, D., Heflin, M. B., and Muellerschoen, R. J. (2002). Examining the C1-P1 Pseudorange Bias. GPS Solutions, 4(4):25–30.*
12. *Kalman, R. E. (1960). A New Approach to Linear Filtering and Prediction Problems. Transactions of the ASME – Journal of Basic Engineering, Series D(82):33–45.*
13. *Kouba J., Heroux P (2001). Precise point positioning using IGS orbit and clock products. GPS Solutions 5(2):12-28.*
14. *Laurichesse, D., Mercier, F., Berthias, J.P., Broca, P., and Cerri, L. (2009). Integer Ambiguity Resolution on Undifferenced GPS Phase Measurements and Its Application to PPP and Satellite Precise Orbit Determination, NAVIGATION: Journal of Institute of Navigation 56(2):135-149.*
15. *Rothacher, M. and Schmid, R. (2006). ANTEX: The Antenna Exchange Format Version 1.3. on-line. Available at ftp://igscb.jpl.nasa.gov/pub/station/general/.*
16. *Tolman, B., R.B. Harris, T. Gaussian, D. Munton, J. Little, R. Mach, S. Nelsen, and B. Renfro (2004). The GPS Toolkit: Open Source GPS Software. Proceedings of the 17th International Technical Meeting of the Satellite Division of the Institute of Navigation ION GNSS 2004, Long Beach, CA, September 21-24, 2004, 2044-2053.*
17. *Schaer, S., Gurtner, W., and Feltens, J. (1998). IONEX: The IONosphere Map Exchange Format Version 1. In Proceedings of the IGS AC Workshop, pages 233–237. ESA/ESOC.*

18. *Schaer, S. and Dach, R. (2008). Model changes made at CODE. IGSMAIL-5771, IGS Central Bureau, Pasadena.*
19. *Seeber, G. (2003). Satellite Geodesy. Walter de Gruyter, Berlin, 2nd edition.*
20. *Welch, G. and Bishop, G. (2006). An Introduction to the Kalman Filter. on-line. Available at: http://www.cs.unc.edu/~welch/media/pdf/kalman_intro.pdf.*
21. *Zumberge J.F., Heflin M.B., Jefferson D.C., Watkins M.M., Webb F.H. (1997). Precise point positioning for the efficient and robust analysis of GPS data from large networks. Journal of Geophysical Research 102(B3):5005-5017.*